Design of an energy efficient transfemoral prosthesis using lockable parallel springs and electrical energy transfer

François Heremans[1] and Renaud Ronsse[1]

Abstract— **Over the last decade, active lower-limb prostheses demonstrated their ability to restore a normal gait for transfemoral amputees by supplying the required positive energy balance [1]. However, the added-value of such devices is significantly impacted by their limited autonomy preventing their full appropriation by the patients. There is thus a strong incentive to reduce the overall power consumption of active prostheses. Addressing this need requires to revisit the electromechanical design. For both the ankle and the knee, the present paper demonstrates that both the use of (un)lockable parallel spring and the transfer of electrical energy between joints can significantly improve the autonomy for overground walking. A simulation model of such a prosthesis was implemented in order to quantify the energy gain being achievable when augmenting a classical series elastic actuator (SEA) with different parallel spring topologies. Simulations predict that adding a lockable parallel spring (LPS) to the SEA reduces the ankle motor consumption by 24% and allows the knee (naturally dissipative) to produce 38% more electrical energy. Moreover, the total energy consumption of the device is reduced to 22J/stride when the harvested electric energy from the knee is stored and transfered to the ankle.**

I. INTRODUCTION

The past decade has seen a lot of research seeking to improve the locomotion capabilities of lower-limb amputees, by providing devices replacing their missing limb and being safe, energy-efficient, and intuitive to use [3][4][5][6]. A related expected impact is to increase the use of lower-limb prosthesis by dysvascular amputees. These strongly disabled patients face tremendous difficulties to use classical prosthesis owing to the challenges associated to (i) providing more energy with the remaining joints [1], (ii) insuring the overall body stability, and (iii) managing the cognitive effort which is required to walk with a passive prosthesis [7]. In addition to these functional objectives, the design of a prosthesis must be guided by several other important criteria: safety, weight, encumbrance, autonomy, comfort and cosmesis (including noise and appearance).

Lower-limb prostheses can be divided into passive and actives devices. The last ones embed actuators that can deliver energy. Only active prosthesis can provide the positive energy balance being required during flat ground walking, and more complex tasks such as slope and stair ascend. This was recently demonstrated in [3] where the authors proved to normalize the gait pattern of transtibial amputees, both regarding kinematics and metabolic cost, using an active device. However, the motorized systems tend to be bulkier and heavier than their passive counterparts. In an effort to reduce weight and encumbrance, existing devices use series elastic actuators (SEA) in order to reduce the motors peak power and thus size, this principle being reviewed in [8].

Yet, active prosthesis are facing another big challenge: autonomy. Although SEA solve the peak power problem, filtering the actuator torque profile is also a desirable target. Indeed, the motor torque is proportional to its current, and the electrical motor losses due to Joule effect are proportional to the square of this current. Consequently, the peak torque directly influences the motor dimensioning, and thus its cost, weight, and potential hazard for the user. In sum, such devices should ideally be both energy efficient, lightweight and sufficiently flexible to accommodate daily life activities outside the lab.

Advanced electro-mechanical design and smart energy management can help to reduce both the battery and motor sizes, and thus weight. Some prosthesis such as [3] (ankle only) embed a parallel spring that engages at late stance allowing the actuator to produce only a fraction of the total joint torque. In [9] a knee module uses a parallel spring that can be actively engaged/disengaged. Some groups further tried to exploit the unbalance in energy production and dissipation of the knee and ankle joints during overground walking. At one extreme, two entirely passive transfemoral prostheses with mechanisms transferring energy from the knee to the ankle during the push-off phase were independently developed in [10] and [11]. More recently, the prostheses developed by the CYBERLGEGs Consortium [5][9] is, to the best of our knowledge, the first combining an passive knee-to-ankle energy transfer mechanism with an active ankle prosthesis [5]. In [12], we explored the design of a prosthesis embedding an infinitely variable mechanical transmission. This requires however that the transmission ratio of such a mechanism can be varied even when the shaft is not rotating. Recently, we developed such a mechanism [13], targeting the transfer and storage of mechanical energy across the joints of an artificial leg. While mechanical energy transfer is only limited by the transmission efficiency, its main challenge relies in storing the energy in a compact form and to transfer it at the appropriate moment.

The prenset work rather focuses on electrical transfer that offers much more freedom regarding the timing of energy delivery. Furthermore, energy can be compactly and silently stored. The main drawback is the electrical conversion efficiency, limited by the motor efficiency itself. Compact and flexible electrical storage of energy has been a challenge for

*This work was supported by the Belgian F.R.S.-FNRS (Aspirant #6809010 awarded to FH).

[1] F. Heremans and R. Ronsse are with the Center for Research in Mechatronics, Institute of Mechanics, Materials and Civil Engineering and Louvain Bionics, Université catholique de Louvain, Belgium.

a long time, but recent advances in the domain of electrolytes open new avenues for active prostheses. More precisely, ultracapacitors are a promising technology, effective for pulsing loads that must be faced by active devices [14][15].

The present work focuses on the development of a new low energy active transfemoral prosthesis using (un)lockable parallel springs and electrical energy transfer between joints. The paper is structured as follows: Section II shows the main characteristic profiles of human overground walking and the resulting design guidelines. Based on such guidelines, Section III describes the proposed new electromechanical design. Section IV then derives a simulation model of this design. The results are then compared and discussed in Section V. The paper ends with a discussion and conclusion.

II. Human walking gait features and related design guidelines

A short overview of the human lower-limb power profile and energy balance during overground walking is first provided, in order to motivate the development of our device.

A. Gait characteristics of human overground walking

The human gait has been thoroughly studied in the literature during the past decades. For instance, data reported in [2] provides useful clues for the design of a device intended to replace a missing limb.

In the sagittal plane, the ankle produces an unidirectional effort gradually increasing during the stance phase, and ending with a high power push-off as shown in Fig. 1 (left). During normal walking, the peak torque of this joint is very high (120Nm for a 75kg individual). This would represent an unfavorable operating point for the electric actuator powering a prosthesis: its efficiency is reduced at high torque/current due to electrical losses.

As depicted in the same Fig. 1 (left), the torque/position curve of the joint can be divided into two phases corresponding to the stance and swing phases respectively. The stance phase is characterized by a stiff response with a net energy production (16J) while the swing phase is dominated by a joint motion with negligible effort. Consequently, a spring with two alternating stiffnesses (high and zero stiffness) can fairly capture this torque/position profile.

The knee also displays a large peak torque at the beginning of the stance phase (Fig. 1 right). During this gait phase, the stiffness of the knee can be very well approximated by a stiff linear spring. This joint further obeys a systematic spring-like negative torque at maximum extension which can be associated with the joint compliant biomechanical limit. Furthermore, the joint is globally dissipative (12J). These observations provide highly valuable guidelines for the design of a low power transfemoral prosthesis.

B. Design guidelines

One way to reduce the actuator torque is to embed passive elastic elements in parallel to the joints (see Fig. 2). When activated at the right time, these passive elements can provide a large amount of the required torque during the stance phase for both joints.

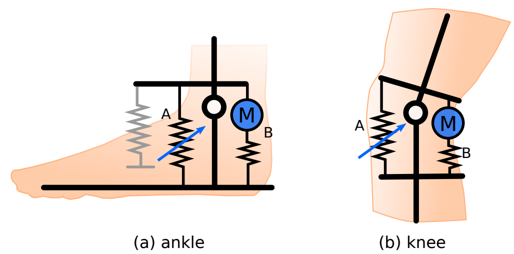

Fig. 2. Dual joints mechanical scheme comprising a variable stiffness parallel spring (A) and a series elastic actuator (B).

Regarding the ankle, a parallel spring can provide a large amount of the required torque as shown in Fig. 3. However, the angle where this spring becomes engaged is critical. Indeed, existing devices typically rely on a fixed stiffness spring engaging only beyond a certain joint angle. This trigger is selected in order to not interfere with the swing phase (trigger 1 in Fig. 3). The contribution of this parallel spring can be enhanced if it engages earlier (trigger 2). However, this generates an undesirable torque profile during the swing phase. Ideally, this would require a parallel spring with a stiffness mimicking the approximation of Fig. 1, i.e. switching between the stance (high stiffness) and swing phases (zero stiffness). The stiffness profile of this

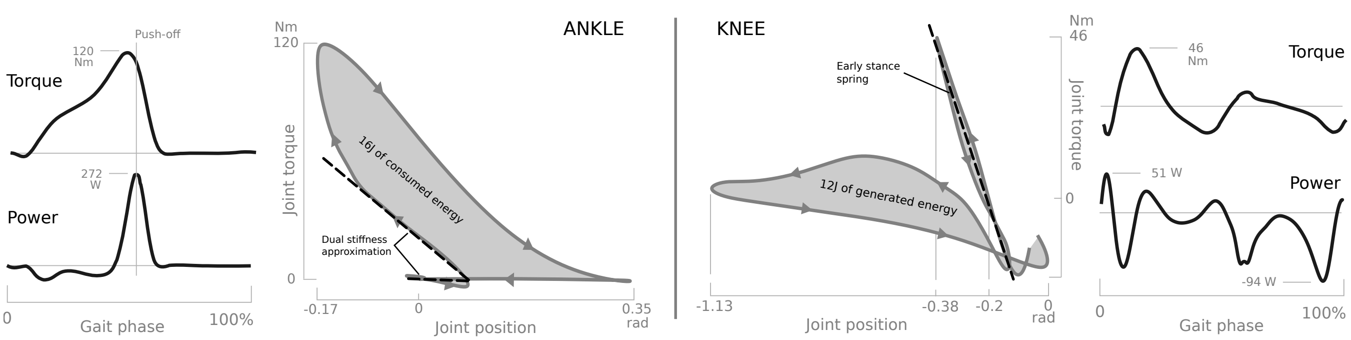

Fig. 1. Ankle: the joint experiences a high peak torque and high peak power. A fraction of the joint torque/position profile can be approximated by two springs with a different stiffness. Knee: the joint experiences a high peak torque and is globally dissipative. The joint torque/position profile can be well approximated by a linear spring during the early stance phase. (Stride length 1.06s and subject mass 75kg, data adapted from [2]).

(un)lockable parallel spring (LPS) is depicted in Fig. 3. At the start of the stance phase, the stiffness of this parallel spring must switch for zero to stiff. In order to trigger at the maximum plantarflexion angle (and thus fully take benefit of the parallel spring), the device should change its stiffness instantaneously, at least at the beginning of the stance phase.

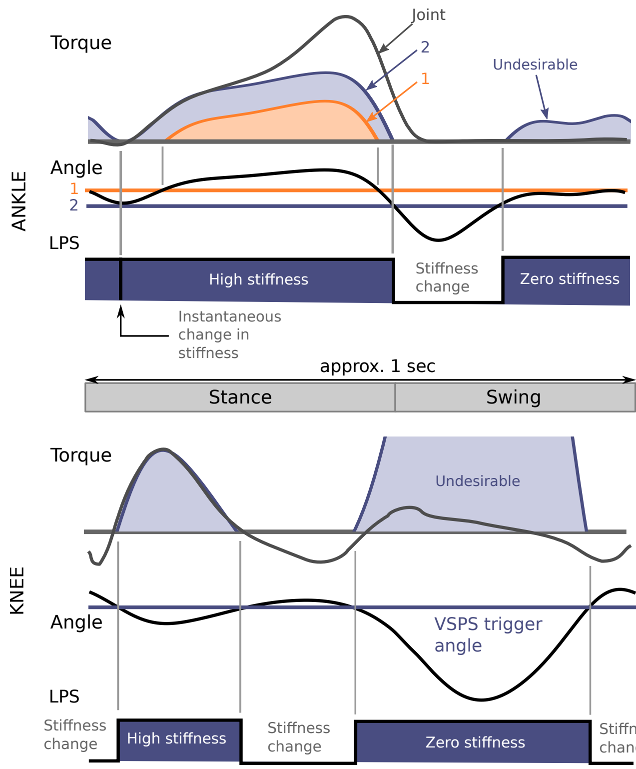

Fig. 3. Torque generated by parallel springs with respect to the joints axis of rotation. For the ankle, existing devices use a fixed stiffness spring (FSS) with a single engagement period, active only during the stance phase (trigger 1). For both joints, the LPS (trigger 2) allows a long engagement period during the stance phase but requires a quick change of stiffness to prevent the generation of undesirable efforts. (The same stiffness is used for both trigger angles in order to facilitate visual comparison.)

Regarding the knee, a dual stiffness system can be used to provide the large linear stiffness at the beginning of the stance phase and then becoming transparent for the late stance and swing phases (see Fig. 3), similarly to [9]. Also, the knee joint being dissipative during the gait cycle, there is an obvious interest to harvest this energy and to store it for later use at the ankle. Such an energy transfer would help to reduce the global power consumption of the integrated transfemoral devices. As we expect to considerably increase the motor efficiency thanks to the LPS, electrical energy transfer becomes competitive to mechanical systems for a much smaller encumbrance and noise via new high density storage technologies.

III. A NEW LOW POWER DEVICE

This section explores the design of a transfemoral prosthesis combining variable stiffness parallel springs and an energy transfer mechanism.

A. A lockable parallel spring (LPS)

State of the art prostheses already use a combination of a fixed stiffness parallel spring and a series elastic actuator, e.g [3], although the spring usually do not exploit the full elastic range of the ankle. Using such a dual stiffness requires to change the stiffness almost instantaneously while keeping the design light. Facing such challenges, we propose here a mechanism able to provide a fast change of stiffness with limited encumbrance.

An overcenter mechanism (arching effect) can be used to very quickly (un)lock the parallel spring anchor position within the gait cycle (see Fig. 4). By nature, this system offers to dynamically set the LPS trigger angle which can vary from one stride to another. The system instantaneously locks at the maximum plantarflexion angle following heel strike for the ankle, and maximum extension for the knee.

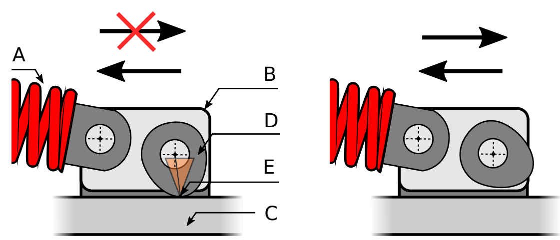

Fig. 4. Overcenter locking mechanism. The spring (A) is anchored to a carriage (B) freely moving linearly on a rail (C). An ellipsoid part (D), comes in contact with the rail (E) to form an overarching configuration (due to the friction cone) guaranteeing locking in one direction. When unloaded, the ellipsoid rotates so that free movement is again possible. Such a mechanism could be used to (de)activate the parallel spring during the stance/swing phase.

The complete stride is depicted in Fig. 5. For the ankle, after heel contact, the parallel spring is placed in the locked position, but can still move freely in one direction to reach the maximum plantarflexion position occuring at the beginning of the stance phase. The spring is then loaded until push-off. At this moment, the mechanism is unloaded and the parallel spring is disengaged to produce an effortless dorsiflexion during the swing phase. For the knee, the mechanism is activated at the end of the swing phase so that the knee is stiff for load bearing. After the initial load, the mechanisms unlocks allowing free knee flexion.

B. Transferring energy between joints

Since we worked for improving the motor efficiency by limiting the peak torque with a LPS, electrical transfer of energy across joints becomes competitive with mechanical systems. This section provides a possible architecture for electrical energy transfer. The energy from the knee is generated at relatively high power (see Fig. 1). Therefore, it requires a storing medium that can withstand a large charging power. Ultracapacitors are perfectly suited for this and can further be used in parallel to the main battery pack. Fig. 6 shows the sketch of such a power supply circuit. A classical LiPo battery pack generates the adequate supply voltage. A power diode prevents any current from flowing back into

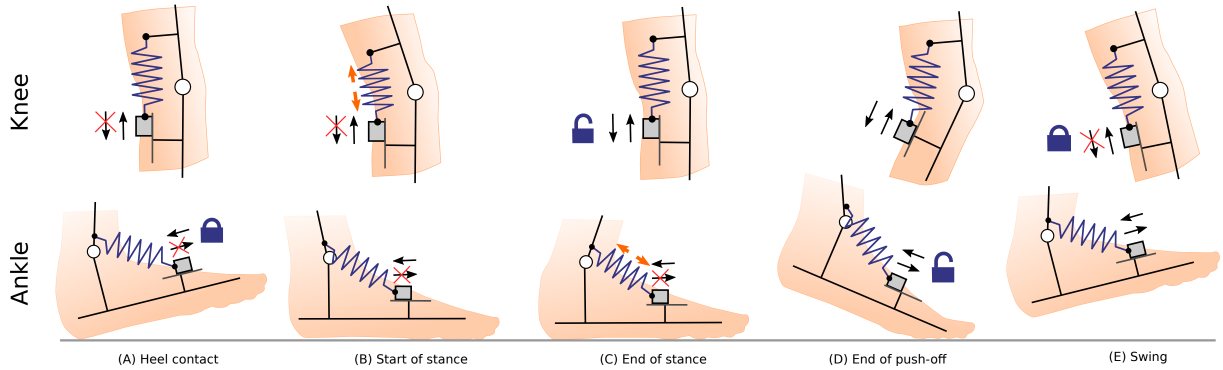

Fig. 5. Gait sequence with the lockable parallel springs. Ankle: (A) At heel contact, the overcenter mechanism toggles in the locked position but allows free movement in plantarflexion (B). (C) During the stance phase, the parallel spring, with its anchor being locked, engages. (D) The parallel spring discharges at push-off and the overcenter mechanism toggles in the unlocked position. (E) The foot executes the swing phase freely. Knee: the overcenter mechanism toggles at the end of the swing phase (E) allowing stiff load bearing (B) and then unlocks (C) before knee flexion.

the pack. A compact ultracapacitor cell is used as a buffer to absorb any negative power. Since ultracapacitors have a low maximum voltage, a fixed gain boost converter (voltage elevation circuit) is placed between the capacitor and supply bus.

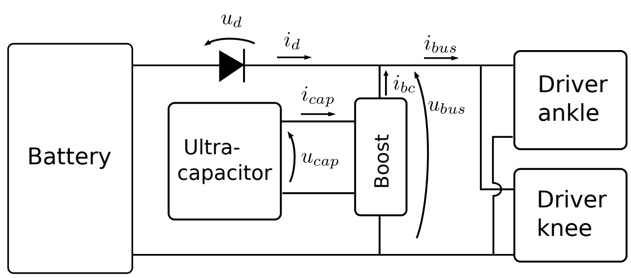

Fig. 6. Power supply system with an unidirectional battery pack and an ultracapacitor.

IV. SIMULATED MODEL

In order to assess the viability of the two proposed design principles (lockable parallel spring and electrical energy transfer), a simulation model is developed. It will further be used to optimize the energy consumption and compare this solution to the state of the art.

A. Mechanical model

For each joint, the torque τ_j and position θ_j trajectories correspond to a normal speed walking in the sagittal plane, taken from [2]. We can thus infer the motor motion dynamics corresponding to theses profiles. Fig. 7 displays the actuator model corresponding to Fig. 2. The joint torque is generated as the summed contributions of a series elastic actuator τ_{ss} and a parallel stiffness mechanism τ_{ps} wich can be engaged and disengaged. The series elastic element has a stiffness K_s and its deformation is computed as the difference between the relative positions of the joint and the motor θ_{mot}. The unidirectional parallel spring has a stiffness K_p, when engaged, and has a rest position angle θ_r.

A mathematical model of the torque would thus be:

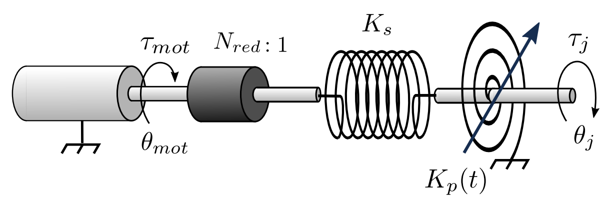

Fig. 7. Joint actuation unit comprising a series elastic actuator (SEA) and a parallel spring which can be engaged and disengaged (LPS).

$$\tau_j = \tau_{ss} + \tau_{ps} \tag{1}$$
$$\tau_{ss} = K_s \cdot (\theta_j - \theta_{mot}/N_{red}) \tag{2}$$
$$\tau_{ps} = K_p \cdot (\theta_r - \theta_j) \cdot \alpha \tag{3}$$
$$\alpha = \begin{cases} 1 & \text{if} \quad (\theta_j < \theta_r) \quad \text{and} \quad \beta = 1 \\ 0 & \text{otherwise} \end{cases} \tag{4}$$

where β is the activation profile different for each joint (see Fig. 3). Indeed, the parallel spring is simulated as a two state system: active with stiffness K_p or inactive with zero stiffness. From the previous equations, the motor position θ_{mot} can be computed as:

$$\theta_{mot} = N_{red} \cdot (\tau_{ss}/K_s + \theta_j) \tag{5}$$
$$\tag{6}$$

In the following, we assume that this quantity is periodic and twice time-differentiable. Under such condition, we can write,

$$\dot{\theta}_{mot} = N_{red} \cdot \left(\dot{\tau}_{ss}/K_s + \dot{\theta}_j\right) \tag{7}$$
$$\ddot{\theta}_{mot} = N_{red} \cdot \left(\ddot{\tau}_{ss}/K_s + \ddot{\theta}_j\right) \tag{8}$$

Because energy consumption is our major concern, efficiency of the mechanical chain η_m must be taken into account. The SEA transmission is modeled by a ball screw (reduction 150:1) and a motor gearhead, so that its whole efficiency is the product of the efficiency of both. A linear interpolation is performed in order to infer the gearhead efficiency η_g as a function of the optimized reduction ratio N_{red}. Values are taken form the catalog of Maxon Motor AG (Sachseln, Switzerland) and range between 50 and 80%. The ball screw transmission efficiency was fixed to $\eta_s = 0.86$, as suggested by guidelines in the catalog of SKF (Göteborg, Sweden). Depending on the direction of the power flow, the total mechanical efficiency has either to be multiplied or divided to the motor torque. In mathematical terms, the motor dynamic equations are thus:

$$\begin{aligned} I \cdot \ddot{\theta}_{mot} &= \tau_{mot} - (\tau_{ss}/N_{red}) \cdot \eta_m && (9) \\ \Leftrightarrow \tau_{mot} &= I \cdot \ddot{\theta}_{mot} + (\tau_{ss}/N_{red}) \cdot \eta_m && (10) \\ \eta_m &= \begin{cases} \frac{1}{\eta_g \cdot \eta_s} & \text{if} \quad p_{ss} = \frac{\tau_{ss} \cdot \dot{\theta}_{mot}}{N_{red}} > 0 \\ \eta_g \cdot \eta_s & \text{otherwise} \end{cases} && (11) \end{aligned}$$

where p_{ss} is the series spring instantaneous power. Here we suppose that the inertia of the system I is dominated by the rotor inertia I_{mot} due to the high reduction ratio being required i.e, $I = \frac{I_{chain}}{N_{red}^2} + I_{mot} \approx I_{mot}$, if $N_{red} \gg 1$. Finally, the model of a simple DC motor model is used, neglecting the motor inductance:

$$\begin{aligned} \tau_{mot} &= K_{mot} \cdot (u_{mot} - K_{mot} \cdot \dot{\theta}_{mot})/R_{mot} && (12) \\ \Leftrightarrow u_{mot} &= \tau_{mot} \frac{R_{mot}}{K_{mot}} + K_{mot} \cdot \dot{\theta}_{mot} && (13) \\ i_{mot} &= \tau_{mot}/K_{mot} && (14) \end{aligned}$$

where K_{mot} and R_{mot} are the motor torque constant and resistance, respectively. Based on the motor torque and speed, we can reconstruct its mechanical p_m and electrical p_e power consumption. The motor maximum efficiency η_{me} is taken into account to compute the electrical power, i.e:

$$\begin{aligned} p_m &= \tau_{mot} \cdot \dot{\theta}_{mot} && (15) \\ p_e &= u_{mot} \cdot i_{mot} \cdot \eta_e && (16) \\ \eta_e &= \begin{cases} \frac{1}{\eta_{me}} & \text{if} \quad u_{mot} \cdot i_{mot} > 0 \\ \eta_{me} & \text{otherwise} \end{cases} && (17) \end{aligned}$$

The total energy provided by the power supply system E_{tot} can be computed numerically, as the sum of the electrical energy of the ankle E_a and the knee E_k.

$$E_a = \int p_{ea}\ dt; \qquad E_k = \int p_{ek}\ dt \tag{18}$$

$$E_{tot} = E_a + E_k \tag{19}$$

B. Power electronics model

The electronic model comprises the motor drivers, the capacitor supply system and the battery pack (see Fig. 6). The chosen state variable is u_{cap}, the voltage across the ultracapacitor. From Eq. 13 and 14, we computed the voltages u_{mot_j} and currents i_j required by each motor. This is further used to compute the motors drivers gains γ_j .

$$\begin{aligned} u_{bus} &= u_{cap} \cdot G_{cap} && (20) \\ \gamma_j &= u_{mot_j}/u_{bus} && (21) \\ i_{bj} &= i_j \cdot \gamma_j && (22) \\ i_{bus} &= \sum_j i_{bj} && (23) \end{aligned}$$

where u_{bus} is the supply bus voltage, G_{cap} is the ultracapacitor DC/DC boost gain and i_{bj} are the motors bus currents of both joints that sum up to give the bus current i_{bus}. The voltage drop across the battery diode u_d can then be computed as the difference between the battery voltage u_{batt} and the bus voltage. When this voltage is larger than the diode forward threshold u_{ft}, the supply current i_d starts flowing through the supply wiring resistance R_s.

$$\begin{aligned} u_d &= u_{batt} - u_{bus} && (24) \\ i_d &= \begin{cases} \frac{u_d - u_{ft}}{R_s} & \text{if} \quad (u_d > u_{ft}) \\ 0 & \text{otherwise} \end{cases} && (25) \end{aligned}$$

The capacitor current i_{cap} is then computed as the difference between the battery current and the bus current taking into account the boost conversion gain and efficiency η_b.

$$\begin{aligned} i_{bc} &= i_{bus} - i_d && (26) \\ i_{cap} &= \begin{cases} G_{cap} \cdot i_{bc}/\eta_b & \text{if} \quad i_{bc} > 0 \\ G_{cap} \cdot i_{bc} \cdot \eta_b & \text{otherwise} \end{cases} && (27) \end{aligned}$$

Eventually, the capacitor voltage can be solved, given the ultracapacitor capacitance C:

$$\frac{du_{cap}}{dt} = -\frac{i_{cap}}{C} \tag{28}$$

C. Computation settings

The parameters K_s, K_p, N_{red} and θ_r are left unknown and a constrained optimization can be performed in order to minimize a weighted sum of the peak power and the electrical energy consumption. Particle Swarm Optimization was chosen to identify the parameters [16]. Feasibility constraints were added to maintain the maximum motor voltage, RMS torque and maximum speed within the motor specifications. Once the optimization succeeded, the electronics model (ordinary differential equation system) was numerically integrated. To guarantee time-differentiability of the input data, a spline (cubic) periodic interpolation was performed. Differentiation was then numerically computed using a centered difference method of order 2. An additional unidirectional parallel spring with a fixed stiffness was added to the knee joint to simulate the biomechanical compliant joint limit at full extension. The stiffness of this spring was equal to K_{p2} and was also part of the optimization. A simple thermal model of the motor was also implemented in order to compute the maximum winding temperature and to guarantee that the motor can sustain continuous operations (during simulated long walking periods). Finally, the torque provided by the parallel spring τ_{ps} was filtered by a running mean filter to capture a smoother engagement as the one generated by (4) and allow differentiation.

To assess the added-value of a LPS, optimizations were performed for both joints for two configurations (a lockable parallel spring and a series elastic actuator – LPS+SEA) and a more basic system (series elastic actuators only – SEA). Another configuration which is relevant for the ankle only was also considered (a parallel fixed stiffness spring engaging at late stance – FSS+SEA). Three different power motors were evaluated: the Maxon EC30 4 poles (200W, 300g), a powerful motor embedded in several prostheses from the literature, e.g [3][4][6] and [17]. the Maxon EC22 4 poles (120W, 170g), being thus lighter; and the Faulhaber BP3274 4 poles (150W, 320g). The main parameters of these motors are given in Table I.

TABLE I
Parameters of the compared motors

Motor	EC30-4p	EC22-4p	BP3274-4p
Rated power [W]	200	120	150
Nominal torque [mNm]	94.6	53.9	111.2
Torque constant [mNm/A]	13.5	10.2	28.4
Resistance [Ohms]	0.102	0.209	0.250
Inertia [gcm²]	33.3	8.91	48
Weight [g]	300	175	320

V. RESULTS

Simulations were performed to assess the quantitative advantage of the proposed mechanism. The optimal mechanical parameters and the associated energetic performance are first reported. The corresponding torque and power profiles are then discussed. As shown in section IV, the power electronics and electro-mechanical models are decoupled such that it can be analyzed separately.

A. Parameters optimization

Optimizations were performed for the three different configurations. The objective was to minimize the energy consumption of the ankle and to maximize the harvested energy at the knee while limiting the motor peak power. Table II and III summarize the optimization results for the ankle and the knee respectively. Note that PSO could not find any solution for the ankle SEA configuration given the constraints related to the tested motors. Indeed, the RMS torque upper bound had to be increased by 20% to 40% to allow a solution to be found and compared. The proposed ankle SEA settings generate winding temperatures reaching the maximum admissible value (155°C) and are thus not sustainable for continuous operations (risk of overheating). A larger motor is required for this configurations, e.g. the Maxon EC32 4 poles.

For the ankle joint, comparing the LPS solution with the SEA alone shows that energy consumption can be reduced

TABLE II
Optimization results for the ankle: energy consumed by the joint (Eq. 19) and optimized parameters.

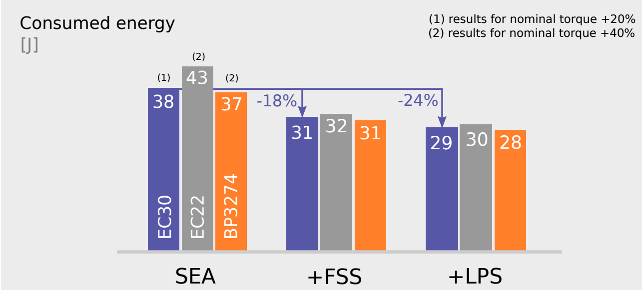

		SEA	+FSS	+LPS	
EC30	P_p	237	347	226	[W]
	K_s	356	1443	201	[Nm/rad]
	K_{red}	728	413	451	[-]
	K_p	-	815	320	[Nm/rad]
	θ_r	-	0.016	0,076	[rad]
EC22	P_p	285	352	236	[W]
	K_s	335	1281	191	[Nm/rad]
	K_{red}	980	720	745	[-]
	K_p	-	798	333	[Nm/rad]
	θ_r	-	0.016	0,076	[rad]
BP32	P_p	250	339	223	[W]
	K_s	337	1392	200	[Nm/rad]
	K_{red}	468	334	359	[-]
	K_p	-	748	324	[Nm/rad]
	θ_r	-	0.016	0.076	[rad]

by 24%. Moreover, the optimal reduction ratio K_{red} is significantly smaller. Compared to the FSS solution, while the LPS consumes only 6% less energy, the peak power P_p and the springs stiffnesses are significantly reduced. The motor choice has little impact on the energy consumption and optimal parameters. The smaller and lighter will thus be preferred.

TABLE III
Optimization results for the knee: energy produced by the joint (Eq. 19) and optimized parameters.

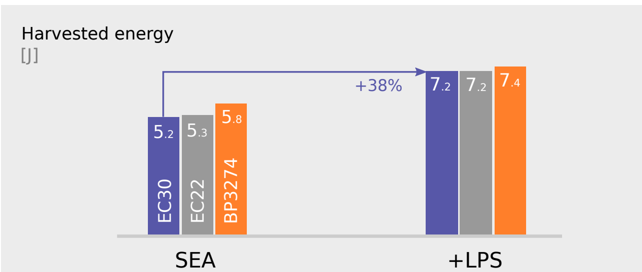

	EC30		EC22		BP32		
	SEA	+VSPS	SEA	+VSPS	SEA	+VSPS	
P_p	100	65	89	66	95	66	[W]
K_s	260	213	274	213	260	207	[Nm/rad]
K_{red}	224	161	402	310	181	131	[-]
K_p	-	376	-	374	-	371	[Nm/rad]
K_{p2}	97	128	100	128	94	126	[Nm/rad]
θ_r	-0.23	-0.23	-0.27	-0.23	-0.23	-0.23	[rad]

For the knee joint, 38% more energy can be harvested when adding a LPS to the SEA+FSS configuration. The peak power and reduction ratio are also largely reduced. Again, the choice of motor does not influence much the results.

B. Torque and power trajectories

The torque and power profiles are reported below, for the configurations embedding an EC30 motor at both joints. Note that the profiles corresponding to the other motors are similar.

As depicted in Fig. 8, using the LPS compared to the purely SEA system leads to a decrease of the motor peak torque by 50% (from 166 to 83Nm). Moreover, the electrical and mechanical power profiles are closer from each other, capturing that less electrical losses are taking place. The peak electrical power is also lowered by 33% (from 352 to 235W). Interestingly, for the FSS optimization, the system lowers the push-off peak torque by converging to a very stiff parallel spring and having the motor and spring working against each other during early stance. The large energy losses of the SEA configuration during late stance is also clearly visible. In all simulations, the difference between the motor torque and the series spring torque is due to the motor inertial torques, during the acceleration/deceleration phases.

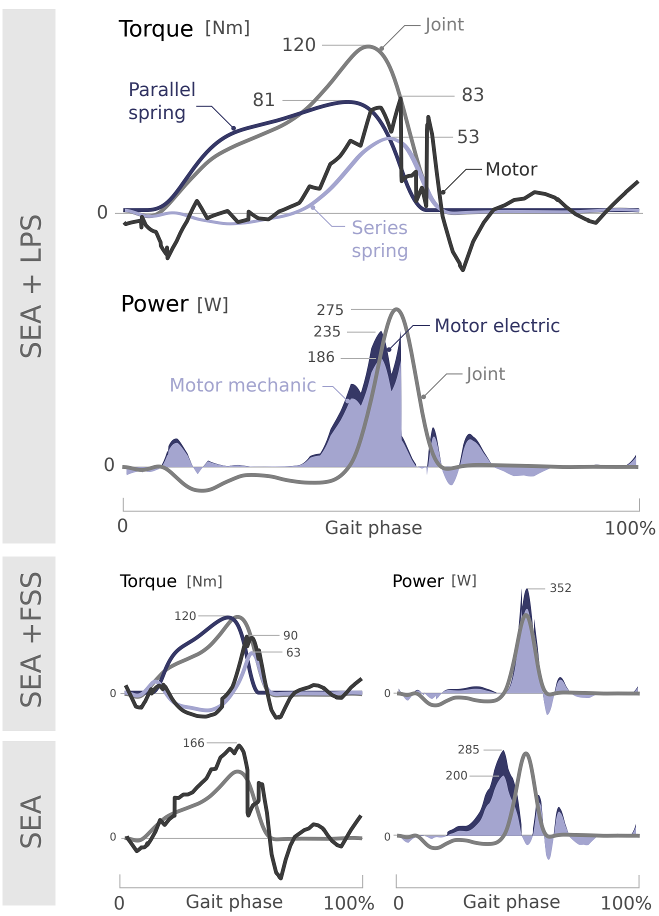

Fig. 8. Torque and power profiles for the ankle over one stride. The SEA+LPS configuration (top) has a 50% lower torque peak than the SEA alone configuration (bottom).

As depicted in Fig. 9, simulations provide similar results for the knee when comparing the LPS and the SEA+FSS configurations: a peak torque reduction of 57% (from 35 to 15Nm) . The power profile shows the reduction in energy losses during early stance and the reduction in peak power.

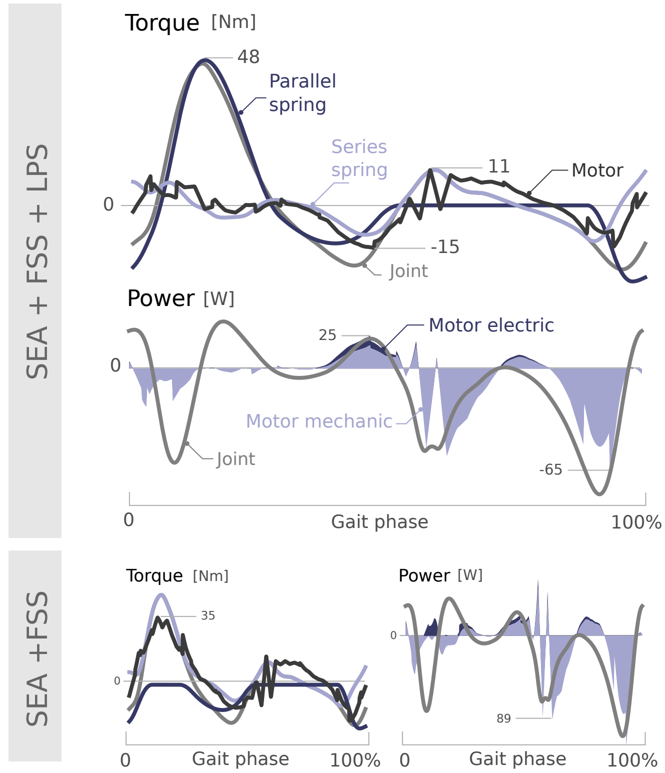

Fig. 9. Torque and power profiles for the knee over one stride. The SEA+LPS configuration (top) has a 57% lower torque peak than the SEA alone configuration (bottom).

C. Power electronics

The power electronics system was simulated for a 24V supply voltage. The ultracapacitor has a 300F capacity, a 2.65V initial charge and DC/DC converter (boost gain) with 95% efficiency. The power supply current profiles are taken at steady state. Adding a LPS provides a 29% decrease in battery RMS current from 1.71A to 1.21A (Fig. 10).

The total energy supplied to the system varies largely as a function of the configurations (see Fig. 11). The total energy consumed when using a LPS on both joints and allowing energy transfer is 22J (the theoretical minimum is 4J, see Fig. 1, so that the global efficiency is about 18%). In comparison, a SEA only configuration with the same energy transfer consumes 33J (i.e. 12% efficiency). Using a LPS thus requires 33% less energy, while using a late stance spring (FSS) brings 21% of energy decrease.

VI. Discussion & Perspectives

The provided results illustrated that the use of a parallel spring that can be (un)locked can greatly improve the power efficiency for both a knee and an ankle prosthesis. Combining a variable stiffness parallel spring with an electronic energy transfer system can further drastically reduce the consumed power of transfemoral devices allowing a much larger autonomy with the same battery pack. Last but not least, a smaller

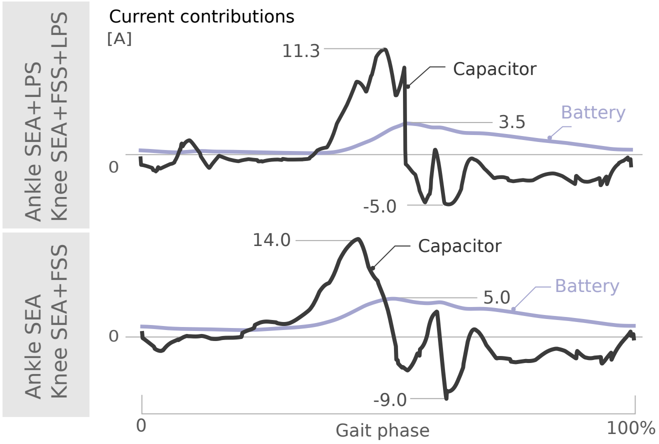

Fig. 10. Current flows in the power supply electronics over one stride. The LPS configuration (top) has a 29% lower rms current than the SEA configuration (bottom).

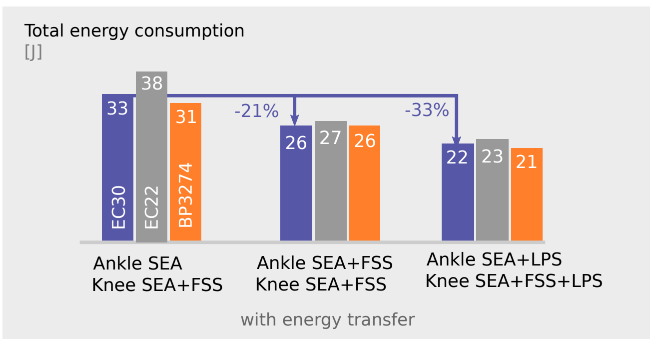

Fig. 11. A large reduction in energy consumption can be achieved using electrical energy transfer and variable stiffness parallel springs.

and lighter motor can be selected, without compromising the task performance. One limitation of this study is the lack of estimating the energy cost of changing the stiffness. However, this change of stiffness occurs when the system is unloaded. A small bistable solenoid could thus be toggled twice per stride to (un)lock the parallel spring. Therefore, the energy expenditure is expected to be negligible in comparison with the joint power motor consumption. Another advantage of such parallel spring is the ability to generate a passive stiffness when the device runs out of power, providing graceful degradation, and thus minimizing the risk of fall. Another desirable feature would be to adapt the stiffness of the parallel spring online according to the walker gait and pace. We are currently considering a mechanism achieving this goal. Eventually, a first prototype of the ankle incorporating the LPS has been designed and is currently being built.

VII. Conclusion

A new transfemoral device was simulated in an effort to design an energy efficient machine. A parallel spring that can be fluently engaged and disengaged was incorporated at both joints to reduce the peak torque and thus largely improve the motor efficiency. An electrical energy transfer mechanism relying on an ultracapacitor was further considered in order to transfer energy from the knee to the ankle. Simulation results showed that, using a LPS and energy transfer, the device total energy consumption can be reduced up to 33% as compared to a classical two joints SEA system with no energy transfer. Future works include the fabrication of a prototype for both joints and a test bench to accurately characterize and measure the energetic performance of the system.

References

[1] R. L. Waters and S. Mulroy, "The energy expenditure of normal and pathologic gait," *Gait & Posture*, vol. 9, no. 3, pp. 207–231, July 1999.

[2] D. A. Winter, *Biomechanics and Motor Control of Human Movement*. John Wiley & Sons, Oct. 2009, google-Books-ID: _bFHL08IWfwC.

[3] H. M. Herr and A. M. Grabowski, "Bionic ankle-foot prosthesis normalizes walking gait for persons with leg amputation," *Proceedings. Biological Sciences / The Royal Society*, vol. 279, no. 1728, pp. 457–464, Feb. 2012.

[4] R. D. Bellman, M. A. Holgate, and T. G. Sugar, "SPARKy 3: Design of an active robotic ankle prosthesis with two actuated degrees of freedom using regenerative kinetics." IEEE, Oct. 2008, pp. 511–516.

[5] J. Geeroms, L. Flynn, R. Jimenez-Fabian, B. Vanderborght, and D. Lefeber, "Ankle-Knee prosthesis with powered ankle and energy transfer for CYBERLEGs α-prototype," *IEEE International Conference on Rehabilitation Robotics: [proceedings]*, vol. 2013, p. 6650352, June 2013.

[6] B. E. Lawson, J. Mitchell, D. Truex, A. Shultz, E. Ledoux, and M. Goldfarb, "A Robotic Leg Prosthesis: Design, Control, and Implementation," *IEEE Robotics & Automation Magazine*, vol. 21, no. 4, pp. 70–81, Dec. 2014.

[7] R. M. Williams, A. P. Turner, M. Orendurff, A. D. Segal, G. K. Klute, J. Pecoraro, and J. Czerniecki, "Does having a computerized prosthetic knee influence cognitive performance during amputee walking?" *Archives of Physical Medicine and Rehabilitation*, vol. 87, no. 7, pp. 989–994, July 2006.

[8] K. Junius, P. Cherelle, B. Brackx, J. Geeroms, T. Schepers, B. Vanderborght, and D. Lefeber, "On the use of adaptable compliant actuators in prosthetics, rehabilitation and assistive robotics," in *ResearchGate*, July 2013, pp. 1–6.

[9] L. Ambrozic, M. Gorsic, J. Geeroms, L. Flynn, R. M. Lova, R. Kamnik, M. Munih, and N. Vitiello, "CYBERLEGs: A User-Oriented Robotic Transfemoral Prosthesis with Whole-Body Awareness Control," *IEEE Robotics Automation Magazine*, vol. 21, no. 4, pp. 82–93, Dec. 2014.

[10] M. Arnout, C. Pierre, V. D. Michael, V. Bram, and L. Dirk, "Concept and design of the HEKTA (Harvest Energy from the Knee and Transfer it to the Ankle) transfemoral prosthesis." IEEE, June 2012, pp. 550–555.

[11] R. Unal, F. Klijnstra, B. Burkink, S. M. Behrens, E. E. G. Hekman, S. Stramigioli, H. F. J. M. Koopman, and R. Carloni, "Modeling of WalkMECH: A fully-passive energy-efficient transfemoral prosthesis prototype." IEEE, June 2013, pp. 1–6.

[12] C. Everarts, B. Dehez, and R. Ronsse, "Variable Stiffness Actuator applied to an active ankle prosthesis: Principle, energy-efficiency, and control." IEEE, Oct. 2012, pp. 323–328.

[13] ——, "Novel infinitely Variable Transmission allowing efficient transmission ratio variations at rest," in *2015 IEEE/RSJ International Conference on Intelligent Robots and Systems (IROS)*, Sept. 2015, pp. 5844–5849.

[14] C. Zhong, Y. Deng, W. Hu, J. Qiao, L. Zhang, and J. Zhang, "A review of electrolyte materials and compositions for electrochemical supercapacitors," vol. 44, no. 21, pp. 7484–7539, Oct. 2015.

[15] A. Kuperman and I. Aharon, "Batteryultracapacitor hybrids for pulsed current loads: A review," *Renewable and Sustainable Energy Reviews*, vol. 15, no. 2, pp. 981–992, Feb. 2011.

[16] J. Kennedy and R. Eberhart, "Particle swarm optimization," 1995.

[17] G. Mathijssen, P. Cherelle, D. Lefeber, and B. Vanderborght, "Concept of a Series-Parallel Elastic Actuator for a Powered Transtibial Prosthesis," *Actuators*, vol. 2, no. 3, pp. 59–73, July 2013.